# Thermodynamic Stability of Neutral and Anionic PFOS: A Gas-Phase, *n*-Octanol, and Water Theoretical Study

**M. Merced Montero-Campillo,[†] Nelaine Mora-Diez,*[,†] and Al Mokhtar Lamsabhi[‡]**

*Department of Chemistry, Thompson Rivers University, Kamloops, British Columbia, V2C 5N3 Canada, and Departamento de Química C-9, Universidad Autónoma de Madrid, Cantoblanco, 28049 Madrid, Spain*

*Received: June 6, 2010; Revised Manuscript Received: July 23, 2010*

The thermodynamic stability of the 89 isomers of the eight-carbon-atom compound perfluorooctane sulfonate (PFOS) in their neutral and anionic forms has been studied in the gas phase, *n*-octanol, and water using density functional theory (B3LYP/6-311+G(d,p)). The gas-phase calculations are compared with previous semiempirical and partial ab initio studies; the calculations in water and *n*-octanol are reported for the first time. The results obtained indicate that the thermodynamic stability assessment of this family of persistent organic pollutants is independent of the environment and type of species (neutral or anionic) considered and that it is important to consider other PFOSs outside of the **83**−**89** set, which is the most frequently studied.

## Introduction

Perfluoroalkyl substances (PFS) have received the interest of the scientific community during the past few years due to their frequent inclusion in the persistent organic pollutants (POP) classification. In particular, perfluoroalkyl sulfonates (PFAS) have received much attention, especially the eight-carbon congeners, the isomers of perfluorooctane sulfonate (PFOS). PFOS can be described with the general formula $C_8F_{17}R$, with $R = SO_3H$ or $SO_3^-$, depending on which species we focus, the neutral (acid form) or the anionic one. The eight perfluorinated carbon atoms can be arranged in 89 structural isomers. To name them, the nomenclature system proposed by Rayne et al. is used in this work.[1]

The most common manufacturing methods of PFS in industry are telomerization and electrochemical fluorination.[2] The latter is the main source of PFOS present in the environment.[3] Due to a lack of deep knowledge about their properties, transport pathways and toxicity,[4] PFOS industrial uses are regulated in the U.S. and have been restricted in the European Union since December 2007.[5] This legal reaction has been motivated by the discovery of some adverse effects caused by PFOS, for example, cancer, neonatal mortality, or defects in laboratory animals. Even though it has been suggested that PFOS levels found in the environment are much lower than the limit representing a real danger to humans, the presence and persistence of PFOS in fetuses, newborn babies, human milk, and human blood has caused alarm. Many toxicological studies have been done in recent years regarding PFOS distribution in human populations, different families of animals, and also rivers, lakes, and oceans around the world.[6−8]

The sulfonate functional group and the strength of the C−F bond are the reasons for the characteristic surfactant behavior of these compounds.[3] They possess hydrophobic and lipophobic molecular regions that allow them to be used as water or oil repellents. In general, PFOSs are soluble in water, have a low volatility, and are not easily adsorbed by organic matter. These features make PFOS nonbiodegradable. Since these compounds

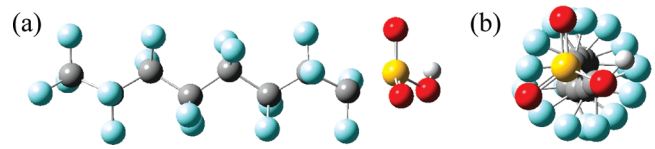


**Figure 1.** Linear neutral PFOS isomer (**89**) in its lowest-energy helical (B3LYP/6-311+G(d,p)) conformation. (a) Lateral view. (b) Axial view.

appear as a mixture of isomers, analytical chemists are currently facing the challenge of having to develop techniques to accurately identify and quantify the different isomers present in a mixture. The percentage of branched and linear isomers is an important question since the completely linear isomer (number **89**; see Figure 1) is the predominant one both in commercial and human blood samples.[9] A recent study investigated the differences in isomer composition of several PFOS derivatives (fluorides, neutral acids, and potassium salts) in several commercial samples using $^{19}$F-NMR. It was found that for the acids, the linear isomer was 72.4% (internally monomethyl branched 17.7%, isopropyl branched 9.4%, and α-methyl branched 3.4%).[9h] Another study performed in Lake Ontario shows that the linear PFOS isomer was 88% of the total mixture (a higher percentage than in technical mixtures),[10] which suggests a quicker natural elimination of the branched isomers. These data reveal the importance of the molecular structure in the bioaccumulation of PFOS.[11]

Taking into account the clear predominance of the linear structure over the branched ones, the question about the thermodynamic stability of the isomers grows in importance; recent studies indicate that it is a matter of discussion if branched isomers are more stable than the linear and less branched isomers. The most abundant presence of the latter in water and biological samples raises important questions. Some authors claim that the linear isomer is the most stable and consequently consider that its predominance in different environments is to be expected. Other authors consider the branched isomers to be of greater thermodynamic stability and explain their absence in the analyzed samples due to the kinetics of their manufacturing process, which does not allow the isomer mixture to reach thermodynamic equilibrium.[12] An in-depth thermodynamic study

* To whom correspondence should be addressed. E-mail: nmora@tru.ca.
[†] Thompson Rivers University.
[‡] Universidad Autónoma de Madrid.

10.1021/jp105187w 
Published on Web 08/24/2010

of the family of isomers both in their neutral and anionic forms is required in order to offer more insight into the origin of PFOS present in the environment and in humans. Such a study could help determine if their origin is by direct discharge or by degradation of other perfluorinated compounds. Furthermore, it would contribute to the theoretical determination of other physicochemical properties of these compounds (e.g., p$K_a$ values and various types of partition coefficients) for which little experimental data exist.[13]

## Computational Details

Electron structure calculations were carried out with the Gaussian03 software package.[14] Density functional theory has been chosen as a reliable and accurate methodology to consider electron correlation, and, in particular, the B3LYP hybrid functional was used with the 6-311+G(d,p) basis set. B3LYP combines the three-coefficient-dependent hybrid functional for the exchange energy proposed by Becke (B3) with the correlation functional proposed by Lee, Yang, and Parr (LYP).[15a,b] All stationary points were characterized as minima by a vibrational frequency analysis using analytical second derivatives. The polarizable continuum model (PCM) using the integral equation formalism variant (IEF-PCM) was used to model solvent effects in the geometry optimizations and frequency calculations performed in *n*-octanol and water.[15c−f] As previously suggested in the literature,[16] calculations in *n*-octanol use a combination of parameters related to this solvent (eps = 9.87, epsinf = 2.043, vmol = 157.625, rsolv = 3.42) and *n*-heptane as the explicitly defined PCM solvent in Gaussian03. All of the calculations using PCM employ the UAHF atomic radii when constructing the solvent cavity.

## Results and Discussion

This is the first ab initio study dedicated to the complete family of the 89 isomers of PFOS in their neutral and anionic forms in the gas phase, n-octanol and water.

Crystallographic and computational studies have shown that the most stable structure for the linear isomer **89** is the helical geometry in which the repulsion between the fluorine atoms is minimized.[12b,17b,c,18] Computational studies on linear perfluorinated alkanes and sulfonamides have reported similar results.[12a,17d] The B3LYP/6-311+G(d,p) gas-phase optimization of PFOS **89**, starting from a fully zigzag conformation, produced a helical conformation which seems to be the global minimum of this isomer in its neutral and anionic form. This geometric disposition can be fully appreciated in its frontal view from the sulfonate head group (see Figure 1b). The remaining isomers (in both the neutral and anionic sets) were initially obtained by systematic substitution on the helical optimized gas-phase framework of PFOS **89**.

**A. Neutral PFOS.** Several previous studies have been devoted to the **83**−**89** isomers,[17] but the only one which has covered the whole family was done by Rayne and co-workers with the PM6 semiempirical method, which does not concur with the conclusions of other authors with respect to the thermodynamic stability of branched and linear PFOS.[12b,d] The Gibbs free energy values obtained by Rayne et al. are given for comparison in Table 1 together with our DFT results in the gas phase, *n*-octanol, and water.

***Stability Order.*** The Gibbs free energy (*G*) difference between the 89 PFOS isomers is remarkable; therefore, it is not surprising that many of them have never been detected in commercial samples or in the environment, independently of the reasons given by the above-mentioned authors in previous works. Calculations in the gas phase indicate that the most (**68**, 1,1′-dimethylhexyl) and the least (**3**, 1-isopropyl-1′,2-dimethylpropyl) stable isomers are 139.6 kJ/mol (more than 33 kcal/mol) apart. This *G* difference is slightly less pronounced in water (137.2 kJ/mol). The same thermodynamic stability ranking for the most and the least stable isomers exists in *n*-octanol and water, with the exception that the most stable isomer (**82**) is 1.1 (in octanol) and 0.2 kJ/mol (in water) more stable than **68**, which is a negligible *G* difference.

In any of the environments considered, the relative *G* values show a large oscillation with the substitution pattern on the main chain. Even though the thermodynamic stability order in neutral PFOS is likely a consequence of the structural changes caused by electrostatic and/or steric repulsive effects due to the abundance of fluorine atoms, the trend observed cannot be easily related to the degree or type of branching. The stability trend seems to be linked to the degree of deviation from the helical conformation of the main chain due to $CF_3$ substitution in certain positions.

It is remarkable that the first six most stable isomers are only separated by 16.5 kJ/mol (less than 4 kcal/mol) in the gas phase and that the energy difference between the three most stable ones (**68**, **82**, **54**) is less than 1 kcal/mol. Therefore, taking into account the inherent approximations of the theoretical methods applied, it is more appropriate to look at general trends in our data rather than the specific stability order associated with the different isomers. If this point of view is taken into account, the apparent randomness of Table 1 is more comprehensible.

A qualitative inspection of Table 1 shows that the least-branched isomers are the most stable ones (four of the seven most stable isomers are in the **82**−**89** group), while the least stable ones (with more than 100 kJ/mol higher in *G* than the most stable isomers) are some of the most-branched isomers (e.g., **3**, **21**, **19**, **26**) with propyl and butyl main chains (see Figure S1, Supporting Information). It is important to note that the linear isomer **89** is the sixth (fifth in water) most stable isomer in the three environments considered, with a difference of 16.5 (14.2 in *n*-octanol and 12.9 in water) kJ/mol from the most stable isomer.

The most stable PFOS isomers in the gas phase are shown in Figure 2, where the stability order decreases in the following order: **68** < **82** < **54** < **48** < **83** < **89** < **88** < **72** < **73**. These isomers share some interesting geometric similarities. All of them are long-chain isomers, and the substituents are located beside of the sulfonic group (e.g., **68**, **54**, **48**, **83**, **72**) or in the tail of the isomer (e.g., **82**, **54**, **48**, **88**, **72**). It seems that methyl substitution in any of these two positions leads to a higher stability. Note that structures **82** and **54** are very similar (the main chain of **82** is one carbon atom longer than that of **54**), and structure **48** is also very close to **54**. Isomers **89** and **88** are also present in the list.

In general, the relative thermodynamic stability of neutral PFOS in the gas phase, *n*-octanol, and water is very similar (see Figures S1−S3, Supporting Information), with mean differences of −0.1 (gas−*n*-octanol and gas−water) and 0.0 kJ/mol (*n*-octanol−water). Interesting correlations are observed between the relative *G* values in the *n*-octanol−gas phase ($R^2$ = 0.998), water−gas phase ($R^2$ = 0.996; see Figure S5, Supporting Information), and water−*n*-octanol ($R^2$ = 0.999; see Figure S4, Supporting Information) data. Details of these correlations are found in Table 2. These correlations are probably present in other families of organic compounds and

**TABLE 1: Relative *G* Values (in kJ/mol at 298.15 K) and Stability Order of the 89 Neutral PFOS Isomers Calculated at the B3LYP/6-311+G(d,p) Level of Theory in the Gas Phase, *n*-Octanol, and Water along with PM6 Calculations in the Gas Phase for Comparison**

| | gas phase | | gas phase | | *n*-octanol | | water | |
|---|---|---|---|---|---|---|---|---|
| PFOS *n* | PM6[a] | | B3LYP/6-311+G(d,p) | | B3LYP/6-311+G(d,p)-PCM | | B3LYP/6-311+G(d,p)-PCM | |
| *n* | Δ*G* | order | Δ*G* | order | Δ*G* | order | Δ*G* | order |
| **1** | 61.5 | 26 | 102.5 | 74 | 105.5 | 75 | 108.0 | 75 |
| **2** | 78.4 | 53 | 107.4 | 76 | 109.0 | 76 | 109.9 | 76 |
| **3** | 83.6 | 60 | 139.6 | 89 | 139.6 | 89 | 137.2 | 89 |
| **4** | 55.3 | 19 | 90.1 | 70 | 93.4 | 71 | 93.9 | 71 |
| **5** | 33.4 | 8 | 83.2 | 63 | 83.9 | 63 | 84.3 | 63 |
| **6** | 70.0 | 41 | 63.0 | 51 | 64.4 | 52 | 65.4 | 53 |
| **7** | 107.3 | 88 | 100.1 | 73 | 101.7 | 73 | 102.3 | 73 |
| **8** | 106.4 | 87 | 93.0 | 72 | 94.5 | 72 | 94.5 | 72 |
| **9** | 62.9 | 28 | 85.1 | 66 | 87.3 | 68 | 86.8 | 65 |
| **10** | 93.7 | 73 | 89.0 | 69 | 89.9 | 70 | 89.2 | 67 |
| **11** | 57.6 | 21 | 46.1 | 35 | 48.8 | 37 | 48.8 | 37 |
| **12** | 106.1 | 86 | 108.9 | 77 | 110.3 | 77 | 111.9 | 77 |
| **13** | 64.0 | 31 | 83.7 | 65 | 86.9 | 66 | 88.5 | 66 |
| **14** | 28.6 | 6 | 47.8 | 36 | 52.3 | 42 | 53.2 | 42 |
| **15** | 100.5 | 81 | 83.3 | 64 | 87.1 | 67 | 90.2 | 69 |
| **16** | 97.0 | 75 | 87.4 | 68 | 86.8 | 65 | 90.0 | 68 |
| **17** | 21.0 | 5 | 45.4 | 33 | 45.0 | 31 | 45.3 | 32 |
| **18** | 67.7 | 38 | 109.2 | 78 | 112.1 | 78 | 121.3[c] | 79 |
| **19** | 102.8 | 84 | 126.8 | 86 | 131.0 | 87 | 131.0 | 87 |
| **20** | 84.0 | 62 | 123.2 | 84 | 124.7 | 84 | 123.8 | 84 |
| **21** | 105.5 | 85 | 129.6 | 88 | 132.7 | 88 | 133.9 | 88 |
| **22** | 78.0 | 51 | 123.1 | 83 | 124.6 | 83 | 125.3 | 85 |
| **23** | 51.2 | 15 | 116.6 | 79 | 119.5 | 80 | 121.1 | 78 |
| **24** | 65.9 | 34 | 79.5 | 60 | 82.5 | 61 | 83.4 | 62 |
| **25** | 0.0 | 1 | 35.7 | 24 | 35.2 | 24 | 35.2 | 24 |
| **26** | 90.8 | 71 | 128.0 | 87 | 129.7 | 86 | 130.8 | 86 |
| **27** | 56.1 | 20 | 122.7 | 82 | 123.2 | 82 | 122.0 | 80 |
| **28** | 67.5 | 37 | 121.1 | 81 | 121.7 | 81 | 123.2 | 83 |
| **29** | 75.6 | 48 | 44.6 | 31 | 46.6 | 33 | 46.3 | 35 |
| **30** | 65.1 | 32 | 58.9 | 47 | 59.1 | 48 | 58.2 | 47 |
| **31** | 46.5 | 14 | 26.6 | 10 | 26.0 | 10 | 25.1 | 9 |
| **32** | 78.4 | 52 | 27.8 | 11 | 28.3 | 15 | 28.6 | 16 |
| **33** | 70.4 | 42 | 58.3 | 46 | 58.9 | 47 | 58.3 | 48 |
| **34** | 60.5 | 23 | 37.9 | 27 | 37.9 | 28 | 36.5 | 27 |
| **35** | 82.4 | 59 | 30.7 | 19 | 30.5 | 20 | 28.8 | 17 |
| **36** | 71.1 | 43 | 72.0 | 56 | 71.6 | 56 | 71.0 | 56 |
| **37** | 108.3 | 89 | 56.8 | 44 | 56.4 | 44 | 56.8 | 45 |
| **38** | 81.4 | 57 | 86.8 | 67 | 85.3 | 64 | 84.4 | 64 |
| **39** | 84.1 | 63 | 58.1 | 45 | 57.0 | 45 | 56.1 | 44 |
| **40** | 101.3 | 83 | 45.4 | 34 | 46.9 | 34 | 45.7 | 33 |
| **41** | 99.8 | 78 | 104.6 | 75 | 103.0 | 74 | 102.5 | 74 |
| **42** | 99.9 | 79 | 74.9 | 59 | 73.0 | 58 | 72.6 | 58 |
| **43** | 68.0 | 39 | 74.8 | 58 | 73.1 | 59 | 72.9 | 59 |
| **44** | 89.7 | 68 | 64.8 | 52 | 65.6 | 53 | 65.1 | 52 |
| **45** | 40.3 | 9 | 79.7 | 61 | 78.7 | 60 | 83.2 | 61 |
| **46** | 30.2 | 7 | 62.6 | 50 | 64.2 | 51 | 64.5 | 51 |
| **47** | 10.1 | 2 | 30.5 | 18 | 30.0 | 19 | 29.3 | 20 |
| **48** | 61.4 | 25 | 5.2 | 4 | 4.4 | 3 | 4.7 | 3 |
| **49** | 79.4 | 56 | 67.0 | 54 | 66.7 | 54 | 67.1 | 55 |
| **50** | 53.8 | 17 | 124.9 | 85 | 126.5 | 85 | 122.2 | 81 |
| **51** | 61.6 | 27 | 60.7 | 49 | 60.6 | 49 | 60.1 | 49 |
| **52** | 65.8 | 33 | 54.2 | 43 | 52.0 | 41 | 52.6 | 41 |
| **53** | 14.4 | 3 | 51.6 | 40 | 53.3 | 43 | 55.1 | 43 |
| **54** | 89.6 | 67 | 3.1 | 3 | 4.5 | 4 | 5.4 | 4 |
| **55** | 63.5 | 29 | 82.7 | 62 | 82.6 | 62 | 82.5 | 60 |
| **56** | 54.6 | 18 | 44.7 | 32 | 46.4 | 32 | 44.3 | 31 |
| **57** | 84.8 | 65 | 90.3 | 71 | 89.8 | 69 | 90.3 | 70 |
| **58** | 98.6 | 76 | 120.0 | 80 | 119.4 | 79 | 122.6 | 82 |
| **59** | 45.3 | 12 | 37.3 | 26 | 36.0 | 25 | 35.7 | 25 |
| **60** | 75.9 | 49 | 73.7 | 57 | 72.1 | 57 | 71.6 | 57 |
| **61** | 61.1 | 24 | 59.9 | 48 | 58.9 | 46 | 57.2 | 46 |
| **62** | 73.9 | 47 | 28.7 | 14 | 29.4 | 17 | 28.9 | 18 |
| **63** | 100.6 | 82 | 44.2 | 30 | 42.5 | 30 | 41.9 | 30 |
| **64** | 73.8 | 45 | 36.2 | 25 | 34.8 | 23 | 33.9 | 23 |
| **65** | 98.9 | 77 | 50.1 | 39 | 48.7 | 36 | 48.2 | 36 |
| **66** | 100.3 | 80 | 52.5 | 41 | 51.3 | 40 | 50.6 | 39 |

**TABLE 1: Continued**

| PFOS *n* | gas phase PM6[a] | | gas phase B3LYP/6-311+G(d,p) | | *n*-octanol B3LYP/6-311+G(d,p)-PCM | | water B3LYP/6-311+G(d,p)-PCM | |
|---|---|---|---|---|---|---|---|---|
| *n* | Δ*G* | order | Δ*G* | order | Δ*G* | order | Δ*G* | order |
| **67** | 90.3 | 70 | 53.1 | 42 | 50.8 | 39 | 50.2 | 38 |
| **68** | 20.1 | 4 | 0.0[b] | 1 | 1.1 | 2 | 0.2 | 2 |
| **69** | 44.9 | 10 | 50.0 | 38 | 50.3 | 38 | 51.0 | 40 |
| **70** | 71.1 | 44 | 34.9 | 23 | 36.6 | 26 | 36.2 | 26 |
| **71** | 52.0 | 16 | 28.4 | 12 | 27.0 | 12 | 26.5 | 12 |
| **72** | 44.9 | 10 | 20.2 | 8 | 19.1 | 8 | 18.7 | 8 |
| **73** | 63.8 | 30 | 26.2 | 9 | 25.1 | 9 | 25.5 | 10 |
| **74** | 88.7 | 66 | 68.3 | 55 | 66.9 | 55 | 65.7 | 54 |
| **75** | 81.7 | 58 | 39.6 | 29 | 38.6 | 29 | 38.3 | 29 |
| **76** | 69.1 | 40 | 33.3 | 21 | 31.7 | 21 | 31.7 | 21 |
| **77** | 67.3 | 36 | 31.4 | 20 | 29.8 | 18 | 29.0 | 19 |
| **78** | 84.8 | 64 | 65.2 | 53 | 63.7 | 50 | 63.0 | 50 |
| **79** | 73.8 | 46 | 38.8 | 28 | 36.8 | 27 | 38.2 | 28 |
| **80** | 66.0 | 35 | 30.1 | 17 | 28.7 | 16 | 28.2 | 15 |
| **81** | 95.9 | 74 | 48.6 | 37 | 47.1 | 35 | 46.0 | 34 |
| **82** | 45.7 | 13 | 1.6 | 2 | 0.0 | 1 | 0.0 | 1 |
| **83** | 58.5 | 22 | 14.7 | 5 | 13.5 | 5 | 13.1 | 6 |
| **84** | 83.8 | 61 | 33.9 | 22 | 33.6 | 22 | 33.7 | 22 |
| **85** | 79.0 | 54 | 29.0 | 15 | 27.1 | 13 | 27.0 | 14 |
| **86** | 79.0 | 55 | 30.0 | 16 | 27.7 | 14 | 26.8 | 13 |
| **87** | 89.7 | 69 | 28.6 | 13 | 26.7 | 11 | 26.4 | 11 |
| **88** | 77.8 | 50 | 17.9 | 7 | 15.7 | 7 | 15.4 | 7 |
| **89** | 90.8 | 72 | 16.5 | 6 | 14.2 | 6 | 12.9 | 5 |

[a] From ref 12b. [b] $G_{gas}$(PFOS-**68**) = −2627.14915 au. [c] Estimated from a single-point calculation in water ($G_w = E_w + TCG_{gas}$).

could be used to predict data in other environments without facing the computational challenges of the simulation of solvent effects.

It was not possible to obtain an aqueous-phase geometry for PFOS **18**. An estimate of its relative *G* value was obtained from a single-point calculation in water using the gas-phase geometry (121.3 kJ/mol). Using the water−*n*-octanol correlation equation, the relative *G* of PFOS **18** in water is predicted to be 112.5 kJ/mol. This value seems to be more reasonable because for the neutral PFOS, there is little difference between the calculated relative *G* values for a given isomer in the gas phase, water, and *n*-octanol.

Even when the global minimum conformer for every PFOS isomer is optimized, the relative *G* values calculated might show some variation with the basis set used. Previous gas-phase results reported at the B3LYP/6-31++G(d,p) level of theory[12c,17e] for isomers **83**−**89** agree reasonably well with our calculations. The largest difference between the relative *G* values reported in this work and the previous ones[17e,12c] is 5.2 kJ/mol for isomer **84**, and the average difference is 1.2 kJ/mol, which is not significant.

***Comparison with the PM6 Semiempirical Study.*** It is of interest to compare the PM6 thermodynamic stability data reported by Rayne et al.[12b] with our DFT results (see Table 1). The first observation is that the number of coincidences in the prediction of the stability order is almost nill, and only isomer **68** is present in the two lists within the top five most stable isomers. With PM6, isomers **89**−**83** do not occupy any of the most stable positions, in clear contradiction with the DFT calculations. PM6 shows a random behavior in the distribution of the thermodynamic stability and predicts some short isomers with very high stability. The DFT calculations indicate a clearer pattern of correspondence between structure/branching and thermodynamic stability.

Another comparison worth mentioning is that the energy interval between the most and the least stable isomers is much greater at the DFT (139.6 kJ/mol) than at the PM6 (108.3 kJ/mol) level. Furthermore, the second most stable isomer is much closer in energy to the first one at the DFT (1.6 kJ/mol) level than that at the PM6 (10.1 kJ/mol) level. The most notable difference between the PM6 and the DFT results is the absence of isomer **89** (and related ones) in the most stable positions, as obtained by applying the B3LYP functional in the gas phase and in solution. The two sets of relative *G* values do not correlate at all ($R^2 = 0.09$); the mean absolute deviation is 31.1 kJ/mol and the mean deviation ($G_{DFT} - G_{PM6}$) is −8.3 kJ/mol. Figure S5 (Supporting Information) displays the calculated relative *G* values in the gas phase at the two levels of theory.

**B. Deviations from the Helical Structure.** The dihedral angle from $C_1$ to $C_4$ in the linear isomer **89** is around −163°. It is remarkable that in all of the isomers with four to eight carbon atoms in the main chain, this dihedral angle is kept or undergoes a small distortion in 80% of the cases. In 60% of the cases, the angle is kept, and in 20% of the cases, a small distortion of 10−14° takes place. The remaining 20% of the isomers have a considerable distortion from the helical structure, between 25 and 50° depending on the case. It was not possible to find a simple pattern to relate branching and the degree of helical distortion in our data. However, it can be said that the most stable isomers (see Table 1) and most of the isomers with one substituent are not significantly distorted from a helical configuration of the main chain, while the most distorted structures have two or more substituents in the central part of the main chain of five carbons or less.

The electrostatic and steric repulsive effects between the fluorinated carbon atoms attached to the main chain lead to distortions from a helical conformation. The structures with the largest distortion have the fluorine atoms of neighboring carbon atoms at a distance of 2.5 Å or greater. If the main chain had a helical conformation, this distance would be less than 2.0 Å. Hence, the structural change is a consequence of the previously mentioned repulsions. The helical structure of isomer **89** is a good starting point for the geometry optimization of the

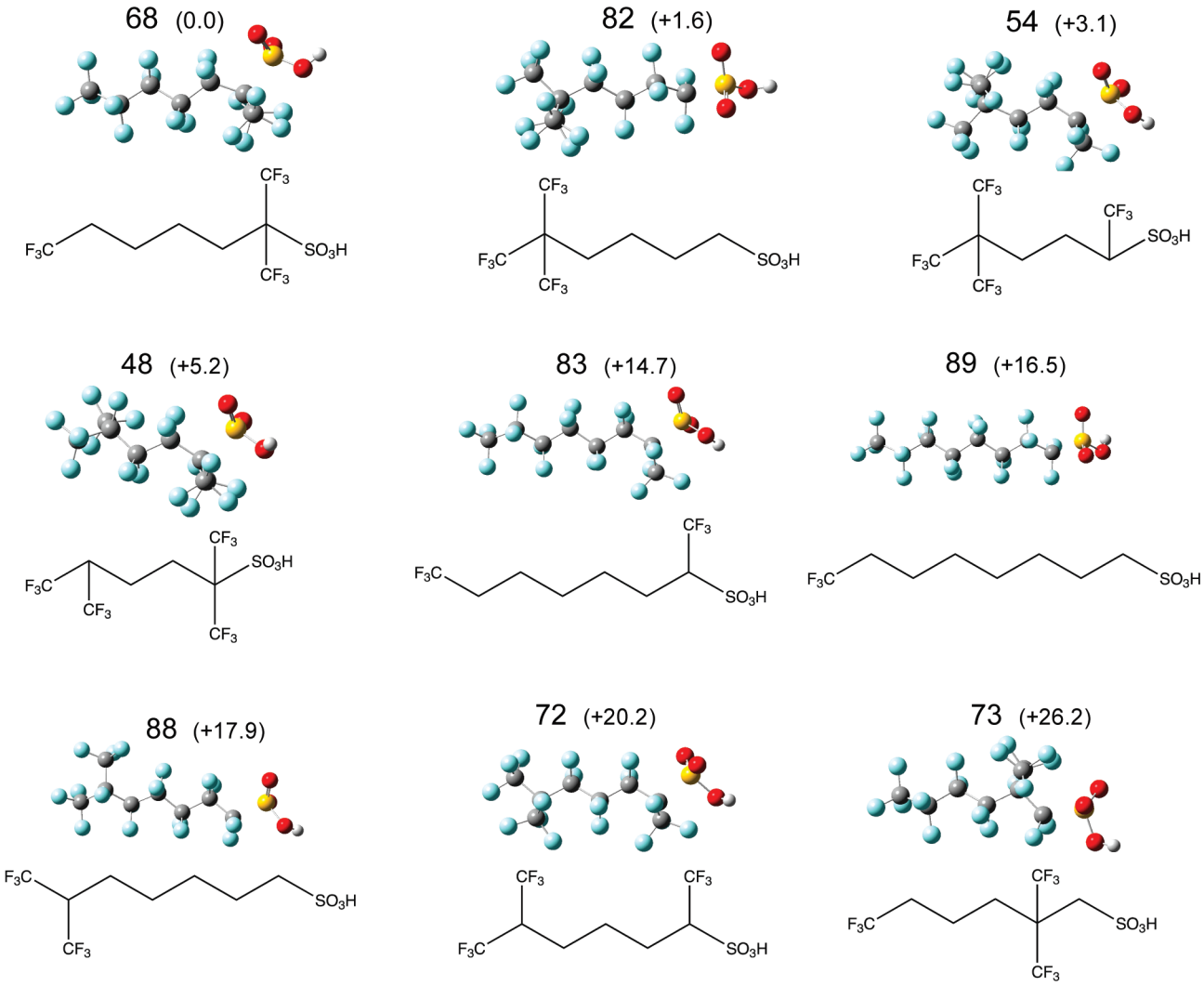


**Figure 2.** Most stable gas-phase neutral isomers with their relative *G* values in kJ/mol at 298.15 K. All main-chain carbons are perfluorinated but depicted as simple carbons for simplicity.

**TABLE 2: Various Correlations[a] between the Relative *G* Values of Neutral and Anionic PFOS in the Gas Phase, *n*-Octanol and Water at 298.15 K along with the Mean of the Differences (in kJ/mol) for Every Pair of Data**

| | $R^2$ | *A* | *B* | mean |
|---|---|---|---|---|
| | | Neutrals | | |
| octanol−gas[b] | 0.998 | 1.023 | −1.292 | −0.1 |
| water−gas | 0.996 | 1.030 | −1.771 | −0.1 |
| water−octanol | 0.999 | 1.008 | −0.515 | 0.0 |
| | | Anions | | |
| octanol−gas[b] | 0.940 | 1.002 | −4.962 | 4.8 |
| water−gas | 0.909 | 0.994 | −6.081 | 6.5 |
| water−octanol | 0.993 | 1.006 | −2.146 | 1.7 |
| | | Neutrals−Anions | | |
| gas phase[c] | 0.805 | 0.962 | −10.656 | −13.4 |
| octanol | 0.939 | 1.016 | −9.625 | −8.5 |
| water | 0.960 | 1.031 | −8.850 | −6.9 |

[a] Square of the correlation coefficient ($R^2$), slope (*A*) and intercept (*B*). [b] $G_{octanol} = AG_{gas} + B$. [c] $G_{neutral-gas} = AG_{anion-gas} + B$.

remaining isomers because the dihedral angle is kept or only slightly distorted in most of the cases, being seriously distorted in those isomers where the repulsion between fluorine atoms forces a different conformation of the main chain.

**C. Anionic PFOS.** The thermodynamic study in the gas phase, *n*-octanol, and water was also performed on the anionic family of PFOS. Previous theoretical studies have only considered the **83**−**89** series of anions.[12d] The calculated relative Gibbs free energy values are displayed in Table 3. Similar to what was found in the study of the neutral isomers, PFOS **68** is the most thermodynamically stable anion in the three environments considered. The second most stable isomer is **48** (with an almost negligible *G* difference of 1.5−2.1 kJ/mol). PFOS **58** is the least stable anion (147.0 kJ/mol) in the gas phase, while PFOS **21** is the least stable in *n*-octanol (140.7 kJ/mol) and water (139.1 kJ/mol). The relative *G* difference for the anions decreases from the gas phase to water (see Table 3). This is to be expected because charged species are more stabilized due to solvation as the polarity of the environment increases.

The three and six most stable anions are within 20.8−13.7 and 24.7−26.0 kJ/mol, respectively, which are greater values than those found for the most stable neutral isomers in the gas phase, *n*-octanol, and water. The stability order in the gas phase decreases in the sequence **68** < **48** < **32** < **54** < **25** < **47**. In *n*-octanol and water, the sequence of the six most stable anions is **68** < **48** < **54** < **82** < **83** < **32**, which highly resemblances the sequence found for the neutrals, **82** < **68** < **48** < **54** < **83/89**. Figure 3 shows the most stable anionic isomers in water. The same general features previously discussed for the neutrals are seen once again (see Figure 2). The geometric characteristics

**TABLE 3: Relative *G* Values (in kJ/mol at 298.15 K) and Stability Order of the 89 Anionic PFOS Isomers Calculated at the B3LYP/6-311+G(d,p) Level of Theory in the Gas Phase, *n*-Octanol, and Water**

| anions | gas phase | | *n*-octanol | | water | | anions | gas phase | | *n*-octanol | | water | |
|---|---|---|---|---|---|---|---|---|---|---|---|---|---|
| PFOS *n* | B3LYP/6-311+G(d,p)[a] | | B3LYP/6-311+G(d,p)-PCM | | B3LYP/6-311+G(d,p)-PCM | | PFOS *n* | B3LYP/6-311+G(d,p)[a] | | B3LYP/6-311+G(d,p)-PCM | | B3LYP/6-311+G(d,p)-PCM | |
| *n* | $\Delta G$ | order | $\Delta G$ | order | $\Delta G$ | order | *n* | $\Delta G$ | order | $\Delta G$ | order | $\Delta G$ | order |
| **1** | 90.3 | 61 | 101.7 | 72 | 105.2 | 75 | **46** | 50.2 | 20 | 57.0 | 35 | 59.9 | 40 |
| **2** | 89.3 | 60 | 99.4 | 71 | 102.9 | 72 | **47** | 24.7 | 6 | 27.2 | 7 | 26.5 | 7 |
| **3** | 113.7 | 77 | 124.5 | 80 | 128.6 | 81 | **48** | 1.5 | 2 | 2.1 | 2 | 1.8 | 2 |
| **4** | 87.9 | 59 | 93.1 | 66 | 93.8 | 67 | **49** | 82.2 | 53 | 79.7 | 55 | 78.2 | 53 |
| **5** | 87.2 | 58 | 89.3 | 62 | 89.5 | 63 | **50** | 133.4 | 84 | 132.8[b] | 84 | 129.5 | 83 |
| **6** | 53.4 | 23 | 59.9 | 38 | 61.8 | 45 | **51** | 73.6 | 46 | 69.3 | 49 | 66.1 | 48 |
| **7** | 109.2 | 75 | 109.5 | 76 | 107.1 | 76 | **52** | 71.9 | 45 | 65.7 | 43 | 62.3 | 46 |
| **8** | 109.4 | 76 | 105.6 | 74 | 103.1 | 73 | **53** | 69.5 | 43 | 63.4 | 42 | 59.5 | 39 |
| **9** | 68.2 | 41 | 76.0 | 52 | 79.2 | 55 | **54** | 21.8 | 4 | 13.7 | 3 | 13.4 | 3 |
| **10** | 93.3 | 64 | 96.2 | 69 | 96.0 | 68 | **55** | 101.1 | 69 | 93.7 | 67 | 90.3 | 64 |
| **11** | 49.6 | 19 | 51.8 | 29 | 51.4 | 31 | **56** | 62.6 | 33 | 56.4 | 34 | 56.0 | 35 |
| **12** | 131.9 | 83 | 126.8 | 81 | 123.6 | 80 | **57** | 115.3 | 78 | 106.1 | 75 | 101.6 | 71 |
| **13** | 71.5 | 44 | 80.6 | 56 | 83.4 | 59 | **58** | 147.0 | 89 | 138.0 | 87 | 134.0 | 86 |
| **14** | 41.0 | 13 | 47.8 | 26 | 50.4 | 30 | **59** | 68.2 | 40 | 55.3 | 32 | 50.1 | 29 |
| **15** | 87.2 | 57 | 91.3 | 64 | 92.0 | 66 | **60** | 103.7 | 72 | 90.6 | 63 | 84.8 | 61 |
| **16** | 96.0 | 67 | 97.2 | 70 | 96.4 | 69 | **61** | 92.2 | 63 | 77.2 | 53 | 71.1 | 51 |
| **17** | 53.9 | 24 | 55.9 | 33 | 54.7 | 34 | **62** | 39.4 | 11 | 35.9 | 12 | 33.1 | 12 |
| **18** | 95.2 | 66 | 102.5 | 73 | 104.4 | 74 | **63** | 73.8 | 48 | 62.6 | 40 | 56.8 | 37 |
| **19** | 131.7 | 82 | 132.8 | 85 | 131.9 | 85 | **64** | 46.6 | 15 | 41.3 | 17 | 39.1 | 17 |
| **20** | 118.4 | 79 | 122.2 | 79 | 122.5 | 79 | **65** | 79.5 | 49 | 66.9 | 44 | 61.5 | 43 |
| **21** | 145.7 | 88 | 140.7 | 89 | 139.1 | 89 | **66** | 83.0 | 55 | 67.3 | 46 | 61.8 | 44 |
| **22** | 140.8 | 87 | 136.7 | 86 | 138.7 | 88 | **67** | 84.8 | 56 | 67.2 | 45 | 62.3 | 47 |
| **23** | 102.1 | 70 | 111.1 | 77 | 114.4 | 77 | **68** | 0.0 | 1 | 0.0 | 1 | 0.0 | 1 |
| **24** | 73.7 | 47 | 78.5 | 54 | 82.9 | 58 | **69** | 63.7 | 35 | 59.2 | 37 | 56.4 | 36 |
| **25** | 24.0 | 5 | 29.4 | 8 | 32.6 | 11 | **70** | 55.5 | 25 | 47.0 | 24 | 43.5 | 23 |
| **26** | 139.3 | 86 | 139.6 | 88 | 138.4 | 87 | **71** | 48.5 | 17 | 39.3 | 15 | 35.8 | 14 |
| **27** | 128.0 | 80 | 129.1 | 82 | 129.4 | 82 | **72** | 39.8 | 12 | 30.7 | 9 | 27.3 | 8 |
| **28** | 136.0 | 85 | 131.4 | 83 | 130.4 | 84 | **73** | 52.7 | 22 | 43.3 | 20 | 43.0 | 22 |
| **29** | 34.2 | 8 | 39.8 | 16 | 42.6 | 21 | **74** | 95.0 | 65 | 84.0 | 60 | 82.8 | 57 |
| **30** | 67.1 | 37 | 68.4 | 48 | 56.8 | 38 | **75** | 67.7 | 38 | 55.2 | 31 | 52.7 | 32 |
| **31** | 37.7 | 10 | 36.0 | 13 | 33.4 | 13 | **76** | 62.7 | 34 | 49.5 | 28 | 46.7 | 27 |
| **32** | 20.8 | 3 | 25.5 | 6 | 26.0 | 6 | **77** | 62.5 | 31 | 48.0 | 27 | 45.8 | 25 |
| **33** | 67.9 | 39 | 67.7 | 47 | 66.8 | 49 | **78** | 96.8 | 68 | 81.4 | 57 | 75.7 | 52 |
| **34** | 50.5 | 21 | 47.1 | 25 | 44.4 | 24 | **79** | 69.3 | 42 | 53.3 | 30 | 48.5 | 28 |
| **35** | 42.9 | 14 | 39.0 | 14 | 36.7 | 15 | **80** | 62.5 | 32 | 45.0 | 22 | 40.6 | 18 |
| **36** | 82.9 | 54 | 81.5 | 58 | 80.3 | 56 | **81** | 80.2 | 51 | 62.9 | 41 | 61.1 | 42 |
| **37** | 80.1 | 50 | 74.6 | 51 | 71.2 | 52 | **82** | 33.3 | 7 | 15.5 | 4 | 14.0 | 4 |
| **38** | 106.6 | 74 | 95.8 | 68 | 91.0 | 65 | **83** | 34.6 | 9 | 24.5 | 5 | 24.2 | 5 |
| **39** | 81.6 | 52 | 73.3 | 50 | 69.9 | 50 | **84** | 61.6 | 28 | 47.0 | 23 | 46.7 | 26 |
| **40** | 64.7 | 36 | 57.6 | 36 | 53.6 | 33 | **85** | 59.5 | 26 | 43.0 | 19 | 41.6 | 20 |
| **41** | 130.3 | 81 | 120.7 | 78 | 116.2 | 78 | **86** | 61.6 | 29 | 43.9 | 21 | 38.7 | 16 |
| **42** | 104.8 | 73 | 91.6 | 65 | 87.0 | 62 | **87** | 60.1 | 27 | 42.2 | 18 | 40.8 | 19 |
| **43** | 102.7 | 71 | 88.9 | 61 | 84.6 | 60 | **88** | 49.3 | 18 | 33.5 | 11 | 30.0 | 10 |
| **44** | 62.4 | 30 | 62.4 | 39 | 61.0 | 41 | **89** | 47.8 | 16 | 31.2 | 10 | 28.5 | 9 |
| **45** | 91.5 | 62 | 83.2 | 59 | 78.6 | 54 | | | | | | | |

[a] $G_{gas}$(PFOS-**68**) = −2626.69183 au. [b] Estimated from a single-point calculation in *n*-octanol ($G_{oct} = E_{oct} + TCG_{gas}$).

of the anions are not substantially different from their related neutral forms, and during the optimization process, a small rearrangement of the molecular structures takes place. The most stable anions are the long-chain isomers with substituents located beside of the sulfonic group or in the tail of the isomer.

The least-branched anionic isomers (**83**−**89**) are not as thermodynamically stable as their neutral counterparts and occupy slightly higher energetic relative positions. The most stable anion in this group, **83**, is 34.6−24.2 kJ/mol from the most stable isomer, occupying the ninth/fifth/fifth position in the gas phase/*n*-octanol/water, while the neutral form is 14.7−13.1 kJ/mol, occupying positions fifth/fifth/sixth.

The linear isomer **89** is the 16th, 10th, and 9th most stable anion in the gas phase, *n*-octanol, and water, respectively, with a difference of 47.8 (31.2 in *n*-octanol and 28.5 in water) kJ/mol from the most stable isomer. In the neutral series, the energy order of this isomer is sixth/sixth/fifth, with an energy difference of 16.5/14.2/12.9 kJ/mol in the three phases considered. However, there are some similarities. PFOS **84**−**87** have very similar relative *G* values, with differences of 2.1/4.8/8.0 kJ/mol in the anions and 5.3/6.9/7.3 kJ/mol in the neutrals.

As in the case of the neutral compounds, previous gas-phase results reported at the B3LYP/6-31++G(d,p) level of theory[12c] for the anions **83**−**89** agree reasonably well with our calculations. The largest difference between the relative *G* values reported in this work and those from the previous one[12c] is 5.8 kJ/mol for isomer **84**, and the average difference is 2.5 kJ/mol, which is not significant.

In general, as in the case of the neutral PFOS, the relative thermodynamic stability of the anionic PFOS in the gas phase, *n*-octanol, and water is very similar (see Figures S6−S8, Supporting Information), with mean differences of 4.8 (gas−*n*-octanol), 6.5 (gas−water), and 1.7 kJ/mol (*n*-octanol−water). Furthermore, the trends found in the neutrals and anions in each of the environments considered are also very similar (see Figures S3 and S4, Supporting Information). The correlations between the *G* values of the anions in the different environments (*n*-octanol−gas phase: $R^2 = 0.940$; water−gas phase: $R^2 = 0.909$) are not as good as those found for

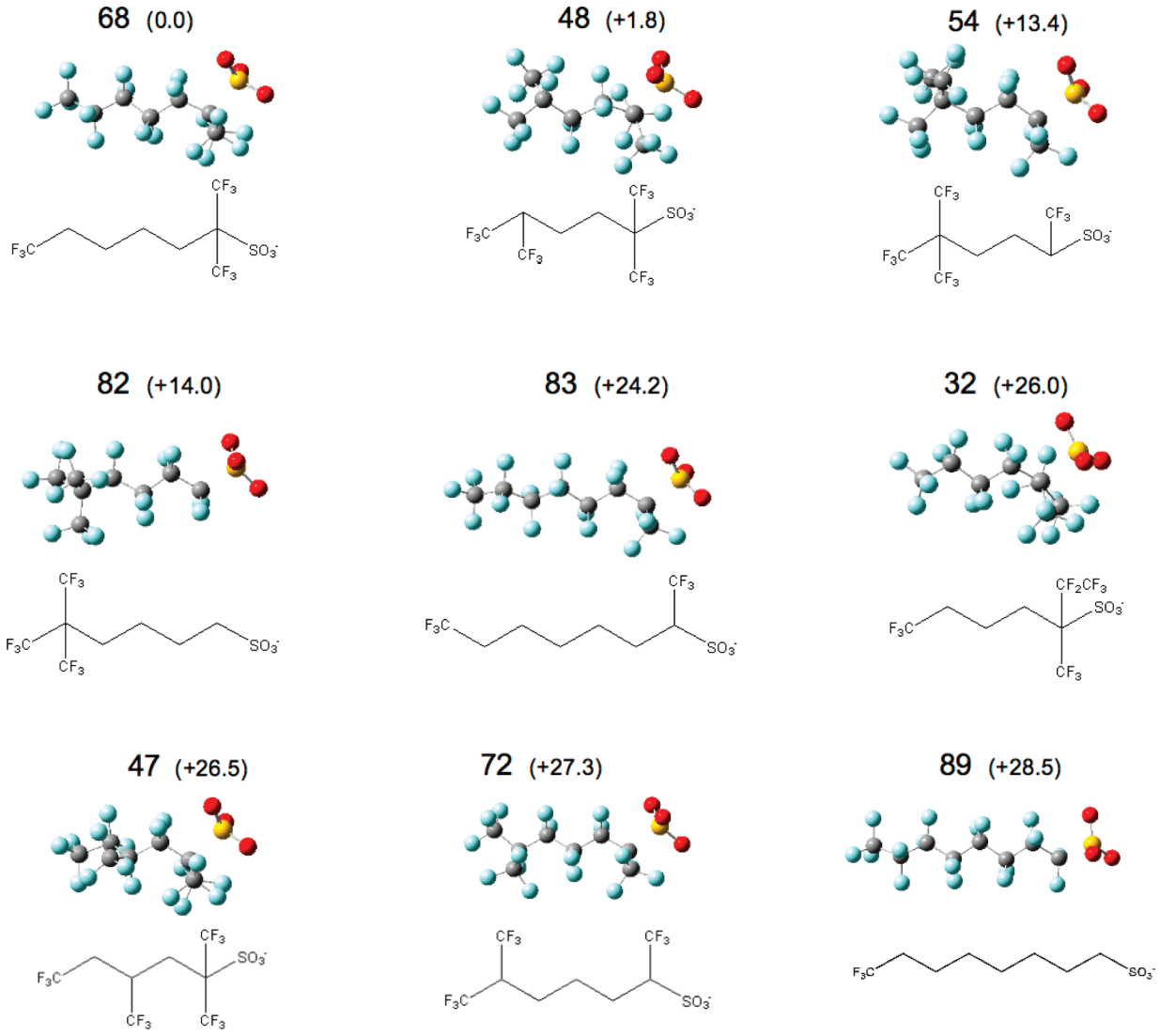


**Figure 3.** Most stable water-phase anionic isomers with their relative *G* values in kJ/mol at 298.15 K. All main-chain carbons are perfluorinated but depicted as simple carbons for simplicity.

the neutral isomers, with the exception of the water−*n*-octanol correlation ($R^2 = 0.993$) (see Table 2) because of the previously commented influence of the charge.

It was not possible to obtain an *n*-octanol geometry for PFOS **50**. An estimate of its relative *G* value was obtained from a single-point calculation in *n*-octanol using the gas-phase geometry (132.8 kJ/mol). Using the water−*n*-octanol correlation equation, the relative *G* of PFOS **50** in *n*-octanol is predicted to be 130.9 kJ/mol.

The correlation between the calculated *G* values for the neutral and anionic PFOS improves as the polarity of the environment increases going from $R^2 = 0.805$ in the gas phase to $R^2 = 0.960$ in water and reflects the small differences in the stability order between the neutral and anionic forms. Figures S9−S11 (Supporting Information) show how the relative *G* values of neutral and anionic PFOS change in the three environments considered. The mean differences go from −13.4 kJ/mol in the gas phase to −8.5 kJ/mol in *n*-octanol and −6.9 kJ/mol in water.

**D. Controversy about the Origin of the PFOS Found in the Environment.** After careful revision of the data obtained, our main conclusion is that the presence of the linear isomer **89** and some of the monomethyl isomers in standard samples and lake waters is not in contradiction with the thermodynamic stability predicted for these species at the DFT level in solution. However, this observation does not necessarily contradict the suggestion of Rayne and co-workers about the origin of the isomers present in various samples. They argue that the overwhelming presence of isomer **89** is not driven by its thermodynamic stability but by the kinetics of the manufacturing procedure followed. Their argument also makes sense because isomers such as **48** and **54**, very close in stability to **89** according to our results, have not been found in standard samples. Hence, to the best of our understanding, this seems to be a reasonable justification of their hypothesis.

## Conclusions

A systematic ab initio study of the thermodynamic stability of the complete family of PFOS isomers in their neutral and anionic forms in the gas phase, *n*-octanol, and water has been carried out for the first time. The DFT calculations indicate that the assessment of the relative thermodynamic stability of PFOS is independent of the environment and type of species (neutral or anionic) considered. However, when assessing the thermodynamic stability and the environmental impact of the members of this family of persistent organic pollutants, it is important to consider other PFOSs outside of the **83**−**89** set, which is the most frequently studied.

Our results indicate that there is a thermodynamic preference for the long-chain isomers without substituents in the middle part of the chain, while in general, the shortest isomers (relative to the length of the longest chain containing the head group) are considerably more unstable. The helical structure of isomer **89** is a good starting point for the geometry optimization of the remaining isomers (in both the neutral and anionic forms) because the dihedral angles are kept or only slightly distorted in most of the cases, being seriously distorted in those isomers where the repulsion between fluorine atoms forces a different conformation of the main chain. According to our results, it is reasonable to suggest that the predominant presence of the linear isomer **89** could be related to the kinetic control of the manufacturing process and not to its thermodynamic stability with respect to the other possible isomers.

The data obtained from this study is essential for calculating the p$K_a$ values of the family of PFOS in the various environments considered, as well as various types of partition coefficients of both the neutral and anionic isomers.[13] These physicochemical magnitudes are crucial for understanding how these compounds distribute and get transported between different possible environments.

**Acknowledgment.** The authors are indebted to financial support from the Natural Sciences and Engineering Research Council of Canada (NSERC). Thanks are also due to Information Technology Services at Thompson Rivers University, the Centro de Supercomputación de Galicia (CESGA), and the Centro de Cálculo de la Universidad Autónoma de Madrid (UAM) for computing time. N.M.D. acknowledges a sabbatical fellowship from the Ministerio de Educación of Spain and the Departamento de Química Física Aplicada at UAM. A.M.L. acknowledges financial support from the DGI Project No. CTQ2009-13129-C01 and the Project MADRISOLAR, ref.: S-0505/PPQ/0225 of the Comunidad Autónoma de Madrid. The authors wish to thank Dr. Carles E. Curutchet for useful suggestions.

**Supporting Information Available:** Structures, names, and labeling system used to identify the 89 PFOS isomers and various graphs comparing relative thermodynamic stabilities of PFOS in different environments. This material is available free of charge via the Internet at http://pubs.acs.org.

## References and Notes

(1) Rayne, S.; Forest, K.; Friesen, K. *J. Environ. Sci. Health, Part A: Tox./Hazard. Subst. Environ. Eng.* **2008**, *43*, 1391–1401.

(2) Kissa, E. *Fluorinated Surfactants*, 2nd ed.; Marcel Dekker: New York, 2002.

(3) Tomy, G. T.; Tittlemier, S. A.; Palace, V. P.; Budakowski, W. R.; Braekevelt, E.; Brinkworth, L.; Friesen, K. *Environ. Sci. Technol.* **2004**, *38*, 758–762.

(4) (a) Kissa, E. *Fluorinated Surfactants and Repellents*; Marcel Dekker: New York, 2001. (b) Beach, S. A.; Newsted, J. L.; Coady, K.; Giesy, J. P. *Ecotoxicological Evaluation of Perfluorooctanesulfonate (PFOS)*; Springer: New York, 2006. (c) Conder, J. M.; Hoke, R. A.; Wolf, W. de; Russell, M. H.; Buck, R. C. *Environ. Sci. Technol.* **2008**, *42*, 995–1003. (d) Betts, K. S. *Environ. Health Perspect.* **2007**, *115*, A250–256. (e) Lau, C. *Reprod. Toxicol.* **2009**, *27*, 209–211. (f) D'eon, J. C.; Mabury, S. A. *Environ. Sci. Technol.* **2007**, *41*, 4799–4805. (g) Houde, M.; Martin, J. W.; Letcher, R. J.; Solomon, K. R.; Muir, D. D. G. *Environ. Sci. Technol.* **2006**, *40*, 3463–3473. (h) Giesy, J. P.; Kannan, K. *Environ. Sci. Technol.* **2001**, *35*, 1339–1342. (i) Simcik, M. F.; Dorweiler, K. J. *Environ. Sci. Technol.* **2005**, *39*, 8678–8683. (j) Paul, A. G.; Jones, K. C.; Sweetman, A. J. A. *Environ. Sci. Technol.* **2009**, *43*, 386–390.

(5) (a) *US EPA Draft Risk Assesment of Potential Human Health Effects Associated with PFOA and Its Salts*, U.S. EPA SAB, May 30, 2006; U.S. EPA public docket EPA-SAB-06-006; U.S. EPA: Washington D. C., 2005. (b) *Off. J. Eur. Union* **2006**, *372*, 32−34.

(6) (a) See ref 4f. (b) Kannan, K.; Corsolini, S.; Falandysz, J.; Fillmann, G.; Kumar, K. S.; Loganathan, B. G.; Mohd, M. A.; Olivero, J.; Van Wouwe, N.; Yang, J. H.; Aldous, J. M. *Environ. Sci. Technol.* **2004**, *38*, 4489–4495. (c) See ref 4g. (d) Calafat, A. M.; Kuklenyik, Z.; Caudill, S. P.; Reidy, J. A.; Needham, L. L. *Environ. Sci. Technol.* **2006**, *40*, 2128–2134. (e) So, M. K.; Yamashita, N.; Taniyasu, S.; Jiang, Q.; Giesy, J. P.; Chen, K.; Lam, P. K. S. *Environ. Sci. Technol.* **2006**, *40*, 2924–2929. (f) Tao, L.; Kannan, K.; Wong, C. M.; Arcaro, K. F.; Butenhoff, J. L. *Environ. Sci. Technol.* **2008**, *42*, 3096–4101. (g) Tao, L.; Ma, J.; Kunisue, T.; Libelo, E. L.; Tanabe, S.; Kannan, K. *Environ. Sci. Technol.* **2008**, *42*, 8597–8602. (h) Li, L.; Xu, Z. S.; Song, G. W. *J. Fluorine Chem.* **2009**, *130*, 225–230.

(7) (a) Kannan, K.; Newsted, J.; Halbrook, R. S.; Giesy, J. P. *Environ. Sci. Technol.* **2002**, *36*, 2566–2571. (b) Kannan, K.; Corsolini, S.; Falandysz, J.; Oehme, G.; Focardi, S.; Giesy, J. P. *Environ. Sci. Technol.* **2002**, *36*, 3210–3216. (c) Bossi, R.; Riget, F. F.; Dietz, R. *Environ. Sci. Technol.* **2005**, *39*, 7416–7422. (d) Kannan, K.; Perrotta, E.; Thomas, N. J. *Environ. Sci. Technol.* **2006**, *40*, 4943–4948. (e) Tao, L.; Kannan, K.; Kajiwara, N.; Costa, M. M.; Fillmann, G.; Takahashi, S.; Tanabe, S. *Environ. Sci. Technol.* **2006**, *40*, 7642–7648. (f) Hart, K.; Kannan, K.; Isobe, T.; Takahashi, S.; Yamada, T. K.; Miyazaki, N.; Tanabe, S. *Environ. Sci. Technol.* **2008**, *42*, 7132–7137.

(8) (a) See ref 7c. (b) Ahrens, L.; Barber, J. L.; Xie, Z.; Ebinghaus, R. *Environ. Sci. Technol.* **2009**, *43*, 3122–3127.

(9) (a) Arsenault, G.; Chittim, B.; McAlees, A.; McCrindle, R.; Riddell, N.; Yeo, B. *Chemosphere* **2008**, *70*, 616–625. (b) De Silva, A. O.; Mabury, S. A. *Environ. Sci. Technol.* **2006**, *40*, 2903–2909. (c) See ref 3. (d) Hansen, K. J.; Johnson, H. O.; Eldridge, J. S.; Butenhoff, J. L.; Dick, L. A. *Environ. Sci. Technol.* **2002**, *36*, 1681–1685. (e) Chu, S. G.; Letcher, R. *Anal. Chem.* **2009**, *81*, 4256–4262. (f) Lehmer, H. J. *Chemosphere* **2005**, *58*, 1471–1496. (g) Arsenault, G.; Chittim, B.; Gu, J.; McAlees, A.; McCrindle, R.; Robinson, V. *Chemosphere* **2008**, *73*, S53–S59. (h) Vyas, S. M.; Kania-Korwel, I.; Lehmler, H-J. *J. Environ. Sci. Health, Part A: Tox./Hazard. Subst. Environ. Eng.* **2008**, *43*, 1391–1401.

(10) Houde, M.; Czub, G.; Small, J. M.; Backus, S.; Wang, X.; Alaee, M.; Muir, D. C. G. *Environ. Sci. Technol.* **2008**, *42*, 9397–9403.

(11) (a) Conder, J. M.; Hoke, R. A.; Wolf, W. de; Russell, M. H.; Buck, R. C. *Environ. Sci. Technol.* **2008**, *42*, 995–1003. (b) See ref 4g.

(12) (a) Liu, P.; Goddard, J. D.; Arsenault, G.; Gu, J.; McAlees, A.; McCrindle, R.; Robertson, V. *Chemosphere* **2007**, *69*, 1213–1220. (b) Rayne, S.; Forest, K.; Friesen, K. J. *J. Mol. Struct.: THEOCHEM* **2008**, *869*, 81–82. (c) Torres, F. J.; Ochoa-Herrera, V.; Blowers, P.; Sierra-Álvarez, P. *Chemosphere* **2009**, *76*, 1143–1149. (d) Rayne, S.; Forest, K. *Chemosphere* **2009**, *77*, 1455–1456.

(13) Montero-Campillo, M. M.; Mora-Diez, N. In preparation.

(14) Frisch, M. J.; Trucks, G. W.; Schlegel, H. B.; Scuseria, G. E.; Robb, M. A.; Cheeseman, J. R.; Montgomery, J. A., Jr.; Vreven, T.; Kudin, K. N.; Burant, J. C.; Millam, J. M.; Iyengar, S. S.; Tomasi, J.; Barone, V.; Mennucci, B.; Cossi, M.; Scalmani, G.; Rega, N.; Petersson, G. A.; Nakatsuji, H.; Hada, M.; Ehara, M.; Toyota, K.; Fukuda, R.; Hasegawa, J.; Ishida, M.; Nakajima, T.; Honda, Y.; Kitao, O.; Nakai, H.; Klene, M.; Li, X.; Knox, J. E.; Hratchian, H. P.; Cross, J. B.; Bakken, V.; Adamo, C.; Jaramillo, J.; Gomperts, R.; Stratmann, R. E.; Yazyev, O.; Austin, A. J.; Cammi, R.; Pomelli, C.; Ochterski, J. W.; Ayala, P. Y.; Morokuma, K.; Voth, G. A.; Salvador, P.; Dannenberg, J. J.; Zakrzewski, V. G.; Dapprich, S.; Daniels, A. D.; Strain, M. C.; Farkas, O.; Malick, D. K.; Rabuck, A. D.; Raghavachari, K.; Foresman, J. B.; Ortiz, J. V.; Cui, Q.; Baboul, A. G.; Clifford, S.; Cioslowski, J.; Stefanov, B. B.; Liu, G.; Liashenko, A.; Piskorz, P.; Komaromi, I.; Martin, R. L.; Fox, D. J.; Keith, T.; Al-Laham, M. A.; Peng, C. Y.; Nanayakkara, A.; Challacombe, M.; Gill, P. M. W.; Johnson, B.; Chen, W.; Wong, M. W.; Gonzalez, C.; Pople, J. A. *Gaussian 03*, revision E.01; Gaussian, Inc.: Wallingford, CT, 2004.

(15) (a) Lee, C.; Yang, W.; Parr, R. J. J. *Phys. Rev. B* **1988**, *37*, 785–789. (b) Becke, A. D. *Chem. Phys.* **1993**, *98*, 5648–5652. (c) Miertus, S.; Scrocco, E.; Tomasi, *J. Chem. Phys.* **1981**, *55*, 117–129. (d) Tomasi, J.; Bonaccorse, R.; Cammi, R.; Del Valle, F. J. O. *J. Mol. Struct.: THEOCHEM* **1991**, *234*, 401–424. (e) Tomasi, J.; Bonaccorse, R. *Croat. Chem. Acta* **1992**, *65*, 29–54. (f) Foresman, J. B.; Keith, T. A.; Wilberg, K. B.; Snoonian, J.; Frisch, M. J. J. *J. Phys. Chem.* **1996**, *100*, 16098–16104.

(16) Curutchet, C.; Orozco, M.; Luque, F. J. *J. Comput. Chem.* **2001**, *22*, 1180–1193.

(17) (a) See refs 12b−d and other related works. (b) Erkoc, S.; Erkoc, F. *J. Mol. Struct.: THEOCHEM* **2001**, *549*, 289–293. (c) Zhang, X.; Learner, M. M. *Phys. Chem. Chem. Phys.* **1999**, *1*, 5065–5069. (d) Jang, S. S.; Blanco, M.; Goddard, W. A.; Caldwell, G.; Ross, R. B. *Macromolecules* **2003**, *36*, 5331–5341. (e) Ochoa-Herrera, V.; Sierra-Alvarez, R.; Somogyi, A.; Jacobsen, N. E.; Wysocki, V. H.; Field, J. A. *Environ. Sci. Technol.* **2008**, *42*, 3260–3264.

(18) Lehmler, H.-J.; Rao, V. V. V. N. S. R.; Nauduri, D.; Vargo, J. D.; Parkin, S. *J. Fluorine Chem.* **2007**, *128*, 595–607.

JP105187W